

We are IntechOpen, the world's leading publisher of Open Access books Built by scientists, for scientists

6,900

Open access books available

186,000

International authors and editors

200M

Downloads

Our authors are among the

154

Countries delivered to

TOP 1%

most cited scientists

12.2%

Contributors from top 500 universities



WEB OF SCIENCE™

Selection of our books indexed in the Book Citation Index
in Web of Science™ Core Collection (BKCI)

Interested in publishing with us?
Contact book.department@intechopen.com

Numbers displayed above are based on latest data collected.
For more information visit www.intechopen.com



Performance Analysis of Composite Thermoelectric Generators

Alexander Vargas Almeida,
Miguel Angel Olivares-Robles and Henni Ouerdane

Additional information is available at the end of the chapter

<http://dx.doi.org/10.5772/66143>

Abstract

Composite thermoelectric generators (CTEGs) are thermoelectric systems composed of different modules arranged under various thermal and electrical configurations (series and/or parallel). The interest for CTEGs stems from the possibility to improve device performance by optimization of configuration and working conditions. Actual modeling of CTEGs rests on a detailed understanding of the nonequilibrium thermodynamic processes at the heart of coupled transport and thermoelectric conversion. In this chapter, we provide an overview of the linear out-of-equilibrium thermodynamics of the electron gas, which serves as the working fluid in CTEGs. The force-flux formalism yields phenomenological linear, coupled equations at the macroscopic level, which describe the behavior of CTEGs under different configurations. The relevant equivalent quantities—figure of merit, efficiency, and output power—are formulated and calculated for two different configurations. Our results show, that system performance in each of these configurations is influenced by combination of different materials and their ordering, that is, position in the arrangement structure. The primary objective of our study is to contribute new design guidelines for development of composite thermoelectric devices that combine different materials, taking advantage of the performance of each in proper temperature range and type of configuration.

Keywords: thermoelectric energy conversion, thermoelectric devices, thermodynamic constraints on energy production, thermoelectric figure of merit, thermoelectric optimization, efficiency

1. Introduction

Thermoelectric devices are heat engines, which may operate as generators under thermal bias or as heat pumps. For waste energy harvesting and conversion, thermoelectricity offers quite

appropriate solutions, when temperature difference between heat source and heat sink is not too large. The physics underlying this type of energy conversion is based on the fundamental coupling between electric charge and energy that each mobile electron carries. The coupling strength is given by the so-called Seebeck coefficient or thermoelectric power [1]. The performance of thermoelectric system is usually assessed against the so-called figure of merit [2]: a dimensionless quantity denoted ZT , which combines the system's thermal and electrical transport properties, as well as their coupling at temperature T .

To qualify as a good thermoelectric, a material (semiconductor or strongly correlated) must boast the following characteristics: small thermal conductivity and large electrical conductivity on the one hand, so that, it behaves as a phonon glass—electron crystal system [2], and large thermoelectric power on the other hand. All these properties, which can be optimized, are temperature-dependent, so they may take interesting values only in a particular temperature range. Improvement of thermoelectric devices in terms of performance and range of applications is highly desired, as their conversion efficiency is not size-dependent, and the typical device does not contain moving parts. Much progress in the field of thermoelectricity has been achieved since the early days, which saw the pioneering works of Seebeck [3] and Peltier [4], but decisive improvement of the energy conversion efficiency, typically 10% of the efficiency of ideal Carnot thermodynamic cycle, is still in order.

In a general manner, transport phenomena are irreversible processes: the generation of fluxes within the system, upon which external constraints are applied, are accompanied by energy dissipation and entropy production [5]. Therefore, thermoelectric effects may be viewed as the result of the mutual interaction of two irreversible processes, electrical transport, and heat transport, as they take place [6]. Not too far from equilibrium, these transport phenomena obey linear phenomenological laws; so, general macroscopic description of thermoelectric systems is, in essence, phenomenological. Linear nonequilibrium thermodynamics provides the most convenient framework to characterize the device properties and the working conditions to achieve various operation modes.

A thermoelectric generator (TEG) is under the influence of two potentials: electrochemical (μ_e) and thermal (T); for each of which there is a flux and a force (as shown in examples of **Table 1**). If force is capable of getting the system to state close to equilibrium after perturbation, then the linear regime may characterize the situation, and approximation in this case is the linear response theory (LRT). In this chapter, we will review and discuss these issues considering thermoelectric system composed of different modules: we are particularly interested in the performance analysis of composite thermoelectric generator (CTEG). For this purpose, we will use a framework based on LRT, which allows to derive a set of linear coupled equations, which contain the system's thermoelectric properties: Seebeck coefficient (α), thermal conductivity (κ), and electrical resistivity (ρ), which are combined to form the effective transport parameters of CTEG in different thermal and electrical arrangements.

The present chapter is organized as follows: as thermoelectric conversion results primarily from nonequilibrium thermodynamic processes, a brief overview of some of the basic concepts and tools developed by Onsager [7, 8] and Callen [6] is very instructive, and we will see, that

the force-flux formalism is perfectly suited for a description of thermoelectric processes [9]. Then, we will turn our attention to the physical model of composite thermoelectric generators, deriving and analyzing the figure of merit, the conversion efficiency and maximum output power. The chapter ends with a discussion and concluding remarks.

Variables	Transport coefficient	Expression and name
Particle flux and density	Diffusion coefficient	$\mathbf{J}_N = -D\nabla n$ Fick's law
Energy flux and temperature	Thermal conductivity	$\mathbf{J}_E = -\kappa\nabla T$ Fourier's law
Electrical current density and electric field	Electrical conductivity	$\mathbf{J} = \sigma\mathbf{E} = -\sigma\nabla\varphi$ Ohm's law

Table 1. Linear thermodynamic phenomenological laws—illustrative examples of forces and fluxes.

2. Basic notions of linear nonequilibrium thermodynamics

2.1. Instantaneous entropy

The thermodynamic formulation presented here is that of Callen [10]. To each set of extensive variables associated to a thermodynamic system, there is a counterpart, that is, a set of intensive variables. The thermodynamic potentials are constructed from these variables. At the macroscopic scale, the equilibrium states of a system may be characterized by a number of extensive variables X_i macroscopic by nature. As one may assume that a macroscopic system is made of several subsystems, which may exchange matter and/or energy among themselves, the values taken by the variables X_i correspond to these exchanges, which occur as constraints are imposed and lifted. When constraints are lifted, relaxation processes take place until the system reaches a thermodynamic equilibrium state, for which a positive and continuous function S differentiable with respect to the variables X_i can be defined as follows:

$$S : X_i \mapsto S(X_i). \quad (1)$$

The function S , called entropy, is extensive; its maximum characterizes equilibrium as it coincides with the values that the variables X_i finally assume after the relaxation of constraints. Note, that extensive variables X_i differ from microscopic variables because of typical time scales, over which they evolve: the relaxation time of microscopic variables is extremely fast, while the variables X_i are slow in comparison. To put it simply, relaxation time toward local equilibrium τ_{relax} is much smaller than the time necessary for the evolution toward the macroscopic equilibrium τ_{eq} . Hence, one may define an instantaneous entropy, $S(X_i)$, at each step of the relaxation of the variables X_i . The differential of the function S is as follows:

$$dS = \sum_i \frac{\partial S}{\partial X_i} dX_i = \sum_i F_i dX_i, \quad (2)$$

where each quantity F_i is the intensive variable conjugate of the extensive variable X_i .

2.2. Thermodynamic forces and fluxes

Examples of well-known linear phenomenological laws are given in **Table 1**. These laws establish a proportionality relationship between forces, which derive from potentials, and fluxes. Proportionality factors are transport coefficients, as fluxes are the manifestation of transport phenomena. Indeed, the system's response to externally applied constraints is transport, and when these are lifted, the system relaxes toward an equilibrium state.

Following the introductory discussion of this section, we now see in more detail how these forces and fluxes appear. The notions, which follow, are easily introduced considering the case of a discrete system like, for instance, two separate homogeneous systems initially prepared at two different temperatures and then put in thermal contact through a thin diathermal wall. The thermalization process triggers a flow of energy from one system to the other. So, assume now an isolated system composed of two weakly coupled subsystems, to which an extensive variable taking the values X_i and X_i' , is associated. One has $X_i + X_i' = X_i^{(0)} = \text{constant}$ and $S(X_i) + S(X_i') = S(X_i^{(0)})$. Then, the equilibrium condition reads:

$$\left. \frac{\partial S^{(0)}}{\partial X_i} \right|_{X_i^{(0)}} = \left. \frac{\partial(S + S')}{\partial X_i} \right|_{X_i^{(0)}} = \frac{\partial S}{\partial X_i} - \frac{\partial S'}{\partial X_i'} = F_i - F_i' = 0, \quad (3)$$

as it maximizes the total entropy. Therefore, if the difference $\mathcal{F}_i = F_i - F_i'$ is equal to zero, the system is in equilibrium; otherwise, irreversible process takes place and drives the system to equilibrium. The quantity \mathcal{F}_i is the affinity or generalized force allowing the evolution of the system toward equilibrium. Further, we also introduce the variation rate of the extensive variable X_i , as it characterizes the response of the system to the applied force:

$$I_i = \frac{dX_i}{dt}. \quad (4)$$

The relationship between affinities and fluxes characterizes the changes due to irreversible processes: non-zero affinity yields non-zero conjugated flux, and a given flux cancels, if its conjugate affinity cancels.

In local equilibrium, fluxes depend on their conjugate affinity, but also on the other affinities; so, we see, that there are direct effects and indirect effects. Therefore, the mathematical expression for the flux I_i , at a given point in space and time (\mathbf{r}, t) , shows a dependence on the force \mathcal{F}_i , but also on the other forces $\mathcal{F}_{j \neq i}$:

$$I_i(\mathbf{r}, t) \equiv I_i(\mathcal{F}_1, \mathcal{F}_2, \dots). \quad (5)$$

Close to equilibrium $I_i(\mathbf{r}, t)$ can be written as Taylor expansion:

$$I_k(\mathbf{r}, t) = \sum_j \frac{\partial I_k}{\partial \mathcal{F}_j} \mathbf{F}_j + \frac{1}{2!} \sum_{i,j} \frac{\partial^2 I_k}{\partial \mathcal{F}_i \partial \mathcal{F}_j} \mathcal{F}_i \mathcal{F}_j + \dots = \sum_k L_{jk} \mathcal{F}_k + \frac{1}{2} \sum_{i,j} L_{ijk} \mathcal{F}_i \mathcal{F}_j + \dots \quad (6)$$

The quantities L_{jk} are the first-order kinetic coefficients; they are given by the equilibrium values of intensive variables F_i . The matrix $[\mathcal{L}]$ of kinetic coefficients characterizes the linear

response of the system. Onsager put forth the idea that there are symmetry and antisymmetry relations between kinetic coefficients [6, 7]: the so-called reciprocal relations must exist in all thermodynamic systems, for which transport and relaxation phenomena are well described by linear laws. The main results can be summarized as follows [5]: (1) Onsager's relation: $L_{ik} = L_{ki}$; (2) Onsager-Casimir relation: $L_{ik} = \varepsilon_i \varepsilon_k L_{ki}$; (3) generalized relations: $L_{ik}(\mathbf{H}, \mathbf{\Omega}) = \varepsilon_i \varepsilon_k L_{ki}(-\mathbf{H}, -\mathbf{\Omega})$, where \mathbf{H} and $\mathbf{\Omega}$ denote, respectively, the magnetic field and angular velocity associated with Coriolis field; the parameters ε_i denote the parity with respect to time reversal: if the quantity studied is invariant under time reversal transformation, it has parity +1; otherwise, this quantity changes sign, and it has parity -1.

3. Thermoelectric forces and fluxes

3.1. Coupled fluxes of heat and electrical charges

The thermoelectric effect results from the mutual interference of two irreversible processes occurring simultaneously in the system, namely heat transport and charge carriers transport. The Onsager force-flux derivation is obtained from the laws of conservation of energy and matter:

$$\mathbf{I}_E = \mathbf{I}_Q + \mu_e \mathbf{I}_N, \quad (7)$$

where \mathbf{I}_E is energy flux, \mathbf{I}_Q is heat flux, and \mathbf{I}_N is particle flux. Each flux is the conjugate variable of its potential gradient. Considering the electron gas, correct potentials for particles and energy are μ_e/T and $1/T$, and related forces are as follows: $\mathbf{F}_E = \nabla(1/T)$ and $\mathbf{F}_N = \nabla(-\mu_e/T)$, where μ_e is the electrochemical potential [1]. Then, the linear coupling between forces and fluxes may simply be described by a linear set of coupled equations involving the so-called kinetic coefficient matrix $[\mathcal{L}]$:

$$\begin{pmatrix} \mathbf{I}_N \\ \mathbf{I}_E \end{pmatrix} = \begin{pmatrix} L_{NN} & L_{NE} \\ L_{EN} & L_{EE} \end{pmatrix} \begin{pmatrix} \nabla(-\mu_e/T) \\ \nabla(1/T) \end{pmatrix}, \quad (8)$$

where $L_{NE} = L_{EN}$. Now, to treat properly heat flow and electrical current, it is more convenient to consider \mathbf{I}_Q instead of \mathbf{I}_E . Using $\mathbf{I}_E = \mathbf{I}_Q + \mu_e \mathbf{I}_N$, we obtain:

$$\begin{pmatrix} \mathbf{I}_N \\ \mathbf{I}_Q \end{pmatrix} = \begin{pmatrix} L_{11} & L_{12} \\ L_{21} & L_{22} \end{pmatrix} \begin{pmatrix} -\nabla(\mu_e/T) \\ \nabla(1/T) \end{pmatrix} \quad (9)$$

with $L_{12} = L_{21}$. Since $\nabla(-\mu_e/T) = -\mu_e \nabla(1/T) - 1/T \nabla(\mu_e)$, then heat flow and electrical current read:

$$\begin{pmatrix} \mathbf{I}_N \\ \mathbf{I}_Q \end{pmatrix} = \begin{pmatrix} L_{NN} & L_{NE} - \mu_e L_{NN} \\ L_{NE} - \mu_e L_{NN} & -2L_{NE}\mu_e + L_{EE} + \mu_e^2 L_{NN} \end{pmatrix} \begin{pmatrix} \nabla(-\mu_e/T) \\ \nabla(1/T) \end{pmatrix} \quad (10)$$

with the following relationship between kinetic coefficients:

$$L_{11} = L_{NN}, \quad (11)$$

$$L_{12} = L_{NE} - \mu_e L_{NN}, \quad (12)$$

$$L_{22} = L_{EE} - 2\mu_e L_{EN} + \mu_e^2 L_{NN}. \quad (13)$$

Note, that since electric field derives from electrochemical potential, we also obtain:

$$\mathcal{E} = -\frac{1}{e} \nabla \mu_e. \quad (14)$$

3.2. Thermoelectric transport coefficients

The thermoelectric transport coefficients can be derived from the expressions of electron and heat flux densities depending on applied thermodynamic constraints: isothermal, adiabatic, electrically open or closed circuit conditions. Under isothermal conditions, electrical current may be written in the form:

$$\mathbf{I}_N = \frac{-L_{11}}{T} \nabla(\mu_e). \quad (15)$$

This is expression of Ohm's law, since with $\mathbf{I} = e\mathbf{I}_N$ we obtain the following relationship between electrical current density and electric field:

$$e\mathbf{I}_N = \mathbf{I} = e \frac{-L_{11}}{T} \nabla(\mu_e) = \sigma_T \left(-\frac{\nabla(\mu_e)}{e} \right) = \sigma_T \mathcal{E}, \quad (16)$$

which contains the definition for isothermal electrical conductivity expressed as follows:

$$\sigma_T = \frac{e^2}{T} L_{11}. \quad (17)$$

Now, if we consider the heat flux density in the absence of any particle transport or, in other words, under zero electrical current, we get:

$$\mathbf{I}_N = \mathbf{0} = -L_{11} \left(\frac{1}{T} \nabla(\mu_e) \right) + L_{12} \nabla \left(\frac{1}{T} \right), \quad (18)$$

so that, the heat flux density under zero electrical current, $\mathbf{I}_{Q_{I=0}}$, reads:

$$\mathbf{I}_{Q_{I=0}} = \frac{1}{T^2} \left[\frac{L_{21}L_{12} - L_{11}L_{22}}{L_{11}} \right] \nabla(T). \quad (19)$$

This is Fourier's law, with thermal conductivity under zero electrical current given by:

$$\kappa_I = \frac{1}{T^2} \left[\frac{L_{11}L_{22} - L_{21}L_{12}}{L_{11}} \right]. \quad (20)$$

We can also define the thermal conductivity κ_E under zero electrochemical gradient, that is, under closed circuit conditions:

$$\mathbf{I}_{Q_{E=0}} = \frac{L_{22}}{T^2} \nabla(T) = \kappa_E \nabla(T). \quad (21)$$

It follows, that thermal conductivities κ_E and κ_I are simply related through:

$$\kappa_E = T\alpha^2\sigma_T + \kappa_I. \quad (22)$$

As thermal and electric processes are coupled, the actual strength of the coupling is given by Seebeck coefficient:

$$\alpha \equiv \frac{-\frac{1}{e} \nabla(\mu_e)}{\nabla(T)} = \frac{1}{eT} \frac{L_{12}}{L_{11}}, \quad (23)$$

defined as the ratio of two forces that derive from electrochemical potential for one and from temperature for the other.

The analysis and calculations developed above allow to establish complete correspondence between kinetic coefficients and transport parameters:

$$L_{11} = \frac{\sigma_T}{e^2} T, \quad (24)$$

$$L_{12} = \frac{\sigma_T S_I T^2}{e^2}, \quad (25)$$

$$L_{22} = \frac{T^3}{e^2} \sigma_T S_I^2 + T^2 \kappa_I, \quad (26)$$

so that, expressions for electronic current and heat flow may take their final forms:

$$\mathbf{I}_N = \frac{\sigma_T}{e^2} T \left(-\frac{\nabla(\mu_e)}{T} \right) + \frac{\sigma_T S_I T^2}{e^2} \left(\nabla\left(\frac{1}{T}\right) \right), \quad (27)$$

$$\mathbf{I}_Q = \frac{\sigma_T S_I}{e^2} T^2 \left(-\frac{\nabla(\mu_e)}{T} \right) + \left[\frac{T^3}{e^2} \sigma_T S_I^2 + T^2 \kappa_I \right] \left(\nabla\left(\frac{1}{T}\right) \right). \quad (28)$$

Since $\mathbf{I} = e\mathbf{I}_N$, it follows that:

$$\mathbf{I} = \sigma_T \mathbf{E} - \frac{\sigma_T S_I}{e} \nabla(T), \quad (29)$$

from which we obtain:

$$\mathbf{E} = \rho_T \mathbf{I} + \alpha \nabla(T), \quad (30)$$

where ρ_T is the isothermal conductivity. This is a general expression of Ohm's law.

4. Formulation of physical model for thermoelectric generators

For TEG performance analysis, we have applied the model given by [11, 12], associating thermal circuit for heat transport and electrical circuit for charge carriers transport, see **Figure 1**.

Electrical current and heat flow, I_i and I_{Q_i} , are functions of generalized forces [11], related to differences in voltage, ΔV_i , and temperature, ΔT_i , of thermoelectric generator:

$$\begin{pmatrix} I_i \\ I_{Q_i} \end{pmatrix} = \begin{pmatrix} 1/R_i & \alpha_i(1/R_i) \\ \alpha_i(1/R_i)T & \alpha_i^2(1/R_i)T + K_i \end{pmatrix} \begin{pmatrix} \Delta V_i \\ \Delta T_i \end{pmatrix}, \quad (31)$$

where T is average temperature.

In this model, TEG is characterized by its internal electrical resistance, R , thermal conductance under open electrical circuit condition, K , and Seebeck coefficient, α . Physical conditions assumed for this model are as follows: (i) thermoelectric properties are independent on temperature, (ii) the only electrical resistance taken into account is that of the legs, (iii) there is no thermal contact resistance between the ends of the legs and heat source, and (iv) in this model, doping of the legs (p- or n-type) is not taken into account, so that, TEG can be seen as only one leg.

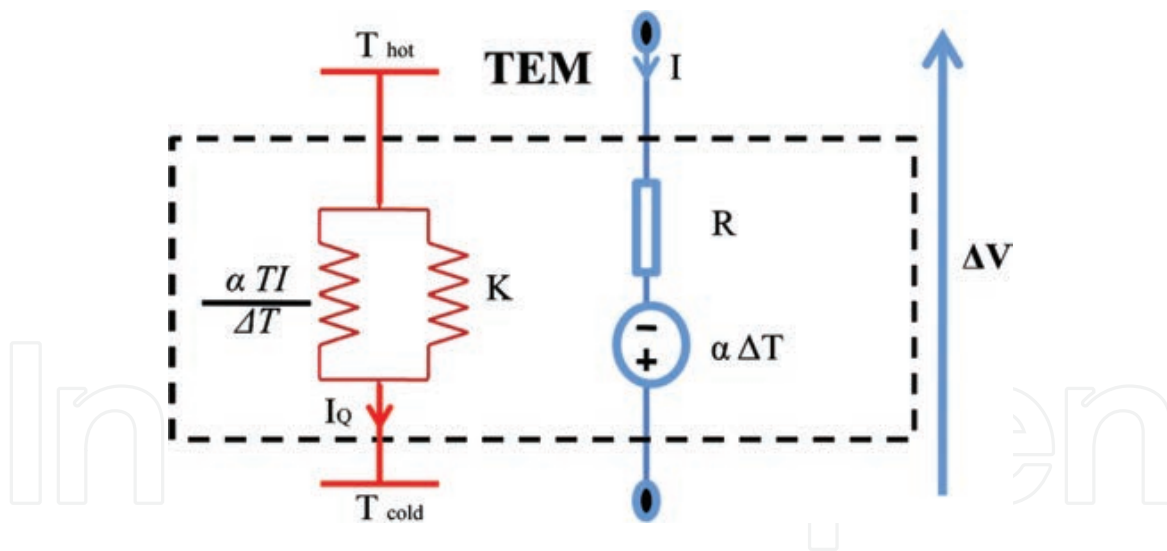


Figure 1. Circuit model for thermoelectric generator, red (thermal circuit), blue (electrical circuit), where ΔV , voltage; R , electrical resistance; K , thermal conductance; T_{cold} , temperature of the cold side; T_{hot} , temperature of the hot side; ΔT , temperature difference; α , Seebeck coefficient; and T , average temperature.

5. Heat balance equation

The heat balance in TEG is governed by the following equations; basically, there are two extreme points: one in contact with the heat source (incoming point):

$$Q_{in} = \alpha T_h I - \frac{1}{2} R_{in} I^2 + K(T_h - T_c), \quad (32)$$

the other point is point, where heat is rejected:

$$Q_{re} = \alpha T_c I + \frac{1}{2} R_{in} I^2 + K(T_h - T_c), \quad (33)$$

where $\alpha T_i I$ is Seebeck heat, $\frac{1}{2} R_{in} I^2$ is Joule heat, and $K(T_h - T_c)$ is thermal conduction heat; in terms of these quantities, electrical power is defined as:

$$P_{electrical} = Q_{in} - Q_{re} = \alpha I(T_h - T_c) - R I^2. \quad (34)$$

6. Composite thermoelectric generator (CTEG)

We consider a composite thermoelectric generator, which is composed of three thermoelectric elements (TEGs) in different configurations, each TEG is made of a different thermoelectric material, see **Figure 2**. The configurations considered are as follows: (A) two-stage thermally and electrically connected in series (TES-CTEG); (B) segmented TEG, conventional TEG, thermally and electrically connected in parallel (PSC-CTEG). Also, we consider the effect of the arrangement of the materials on the performance of the composite system. Thus, for each of the systems (A, B), we have the following arrangements:

- a. TEG 1 = material one, TEG 2 = material two, TEG 3 = material three;
- b. TEG 1 = material three, TEG 2 = material one, TEG 3 = material two;
- c. TEG 1 = material two, TEG 2 = material three, TEG 3 = material one.

In the following sections, we analyze and show results for CTEG by applying the conditions listed above in order to contribute to development of new design guidelines for thermoelectric systems with news architectures and even to provide some clues to the search for new physical conditions in the area of science and engineering of thermoelectric materials.

6.1. Formulation of equivalent figure of merit for CTEG

To analyze CTEG performance, equivalent quantities are defined, which contain the overall contribution of individual properties of each TEG building up composite system. These quantities are as follows: equivalent Seebeck coefficient (α_{eq}), equivalent electrical resistance (R_{eq}), and equivalent thermal conductance (K_{eq}), in terms of which it is possible to have equivalent figure of merit (Z_{eq}). We show the impact of the configuration of the system on Z_{eq} for each of configuration (A, B) listed in Section 6, and we suggest the optimum configuration. In order to justify the effectiveness of the equivalent figure of merit, the corresponding efficiency has been calculated for each configuration.

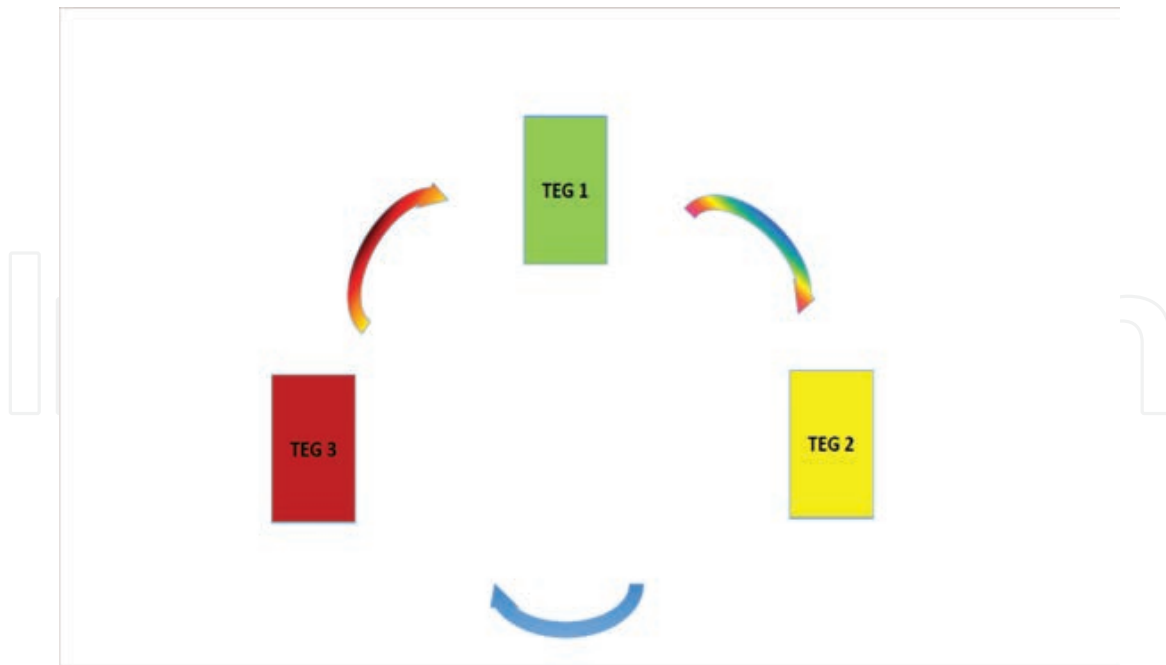


Figure 2. Composite thermoelectric generator (CTEG) (components are three TEGs, each made of different material).

6.1.1. Two-stage thermally and electrically connected in series

Schematic view of this system is shown in **Figure 3**. The first stage (bottom stage) consists of two different thermoelectric modules (TEG), while the top stage consists of only one TEG. Each of components is characterized by proper thermoelectric properties (α_i, R_i, K_i) [13].

Using Eq. (31), the heat flux within any segment in TEGs is:

$$I_{Q_i} = \alpha_i T I_i + K_i \Delta T_i. \quad (35)$$

By continuity of the heat flux through the interface between stages of TES-CTEG:

$$I_{Q1} = I_{Q2} + I_{Q3}$$

$$K_1(T_{hot} - T_i) + \alpha_1 T I = K_2(T_i - T_{cold}) + \alpha_2 T I + K_3(T_i - T_{cold}) + \alpha_3 T I, \quad (36)$$

from which we obtain the average temperature at the interface between stages [12]:

$$T_i = \frac{K_1 T_{hot} + (K_2 + K_3) T_{cold} + (\alpha_1 - \alpha_2 - \alpha_3) T I}{K_1 + K_2 + K_3}. \quad (37)$$

Since all components are electrically connected in series, the total voltage is given by:

$$\Delta V = -\alpha_1(T_{hot} - T_i) - \alpha_2(T_i - T_{cold}) - \alpha_3(T_i - T_{cold}) + (R_1 + R_2 + R_3)I, \quad (38)$$

substituting the value of T_i in the last equation, we have:

$$\Delta V = \left[\frac{-(\alpha_2 + \alpha_3)K_1 - \alpha_1 K_2 - \alpha_1 K_3}{K_1 + K_2 + K_3} \right] [T_{hot} - T_{cold}] + \left[\frac{(\alpha_1 - \alpha_2 - \alpha_3)^2 T}{K_1 + K_2 + K_3} + (R_1 + R_2 + R_3) \right] I. \quad (39)$$

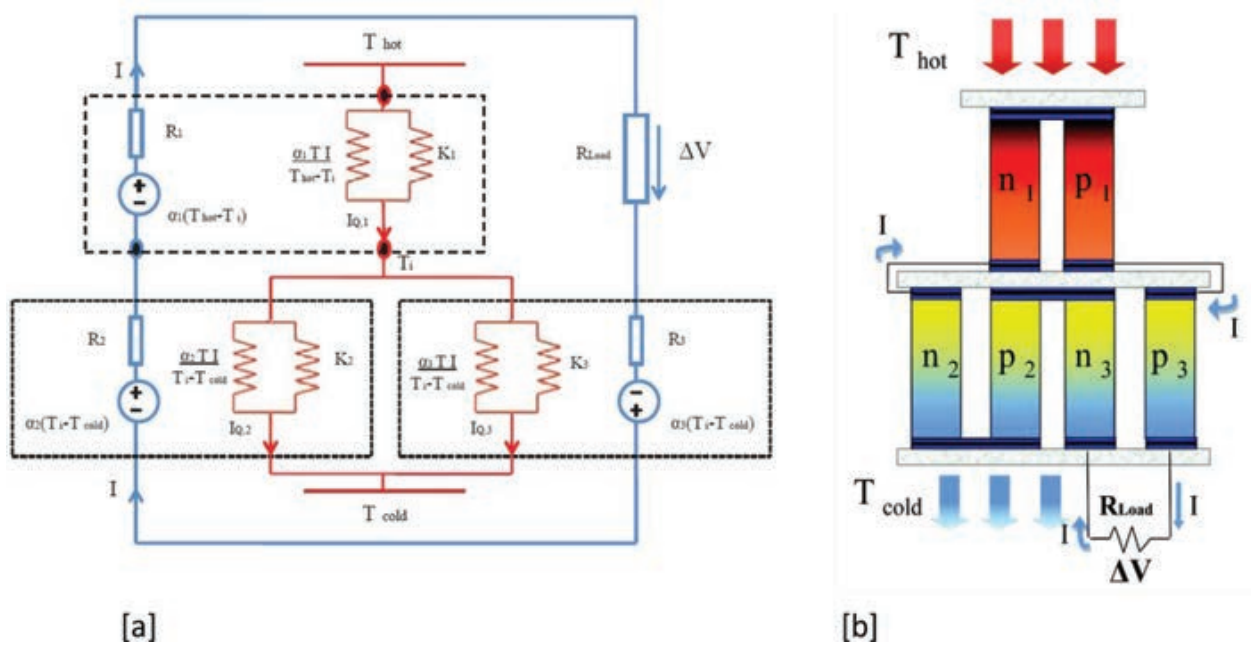


Figure 3. Schematic representation of thermoelectric system composed of two stages thermally and electrically connected in series (TES-CTEG). (a) Equivalent circuit for TES-CTEG, where ΔV is the voltage, R_i is the electrical resistance, K_i is the thermal conductance, T_{cold} is the temperature of the cold side, T_{hot} is the temperature of the hot side, ΔT is the temperature difference, α_i is the Seebeck coefficient, T is the average temperature, R_{load} is the load; (b) practical device related to TES-CTEG, where n_i is the i th n -type material, p_i is the i th p -type material.

From Eq. (39), we identified the equivalent series Seebeck coefficient, α_{eq-TES} , and equivalent series electrical resistance, R_{eq-TES} , as follows:

$$\alpha_{eq-TES} = \frac{-(\alpha_2 + \alpha_3)K_1 - \alpha_1 K_2 - \alpha_1 K_3}{K_1 + K_2 + K_3}, \quad (40)$$

$$R_{eq-TES} = R_1 + R_2 + R_3 + R_{relax}, \quad (41)$$

where

$$R_{relax} = \frac{(\alpha_1 - \alpha_2 - \alpha_3)^2 T}{K_1 + K_2 + K_3}. \quad (42)$$

Considering open circuit condition for the system, $I = 0$, we find, that equivalent thermal conductance for the whole system:

$$K_{eq-TES} = \frac{K_1(K_2 + K_3)}{K_1 + K_2 + K_3}. \quad (43)$$

We define the figure of merit in terms of equivalent quantities [12]:

$$Z_{eq} = \frac{\alpha_{eq}^2}{R_{eq}K_{eq}}. \quad (44)$$

By replacing the results obtained in Eqs. (40)–(43), we have:

$$Z_{eq-TES} = \frac{\left[\frac{-(\alpha_2 + \alpha_3)K_1 - \alpha_1 K_2 - \alpha_1 K_3}{K_1 + K_2 + K_3} \right]^2}{\left[\frac{(\alpha_1 - \alpha_2 - \alpha_3)^2 T}{K_1 + K_2 + K_3} + (R_1 + R_2 + R_3) \right] \left[\frac{K_1(K_2 + K_3)}{K_1 + K_2 + K_3} \right]}. \quad (45)$$

6.1.2. Segmented TEG-conventional TEG thermally and electrically connected in parallel

In this section, we consider CTEG system, which is composed by segmented TEG and conventional TEG. These TEGs are thermally and electrically connected in parallel (PSC-CTEG), as is shown in **Figure 4**.

In the composite system, there are two currents, I_s for TEG 1 and TEG 2, I_c for TEG 3. If the electrical current is conserved, then [13]:

$$I_{eq} = I_s + I_c. \quad (46)$$

The heat flux through the whole system is the sum of the heat flux flowing through segmented generator and the heat flux in conventional generator. Thus:

$$I_{Q-eq} = I_{Q_s} + I_{Q_c}. \quad (47)$$

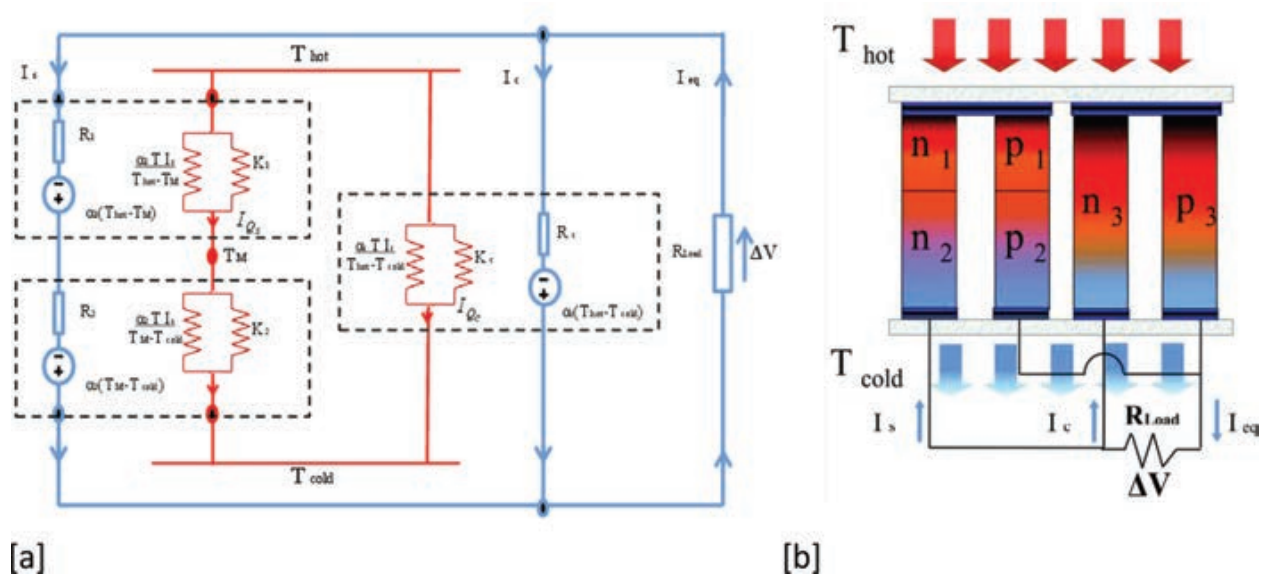


Figure 4. Schematic representation of (PSC-CTEG). (a) Thermal-electrical circuit, where ΔV is the voltage, R_i is the electrical resistance, K_i is the thermal conductance, T_{cold} is the temperature of the cold side, T_{hot} is the temperature of the hot side, ΔT is the temperature difference, α_i is Seebeck coefficient, T is the average temperature, R_{load} is the load resistance, T_M is the intermediate temperature; (b) structure design, where n_i is the i^{th} n -type material, p_i is the i^{th} p -type material.

To obtain the equivalent electrical resistance, R_{eq-PSC} , using Eq. (45), the isothermal condition, $\Delta T = 0$, is required. Under this condition, we recover the usual expression of equivalent electrical resistance for an ohmic circuit. Thus, we get:

$$R_{eq-PSC} = \frac{R_s R_c}{R_s + R_c}, \quad (48)$$

where R_c is the internal electrical resistance of conventional TEG and R_s is the electrical resistance of the segmented TEG:

$$R_s = R_1 + R_2 + R_{relax} \quad (49)$$

and

$$R_{relax} = \frac{(\alpha_1 - \alpha_2)^2 T}{K_1 + K_2}. \quad (50)$$

Assuming the condition of closed circuit, $\Delta V = 0$, and applying Eq. (45), we have for equivalent Seebeck coefficient [13]:

$$\alpha_{eq-PSC} = \frac{R_c \alpha_s + R_s \alpha_c}{R_s + R_c}, \quad (51)$$

where

$$\alpha_s = \frac{K_2 \alpha_1 + K_1 \alpha_2}{K_1 + K_2}. \quad (52)$$

To determine equivalent thermal conductance, K_{eq} , we use the open circuit condition, $I_{eq} = 0$, which is satisfied when $I_s = -I_c = I$, and, due to preservation of heat flow:

$$K_{eq-PSC} = K_s + K_c + \frac{(\alpha_s - \alpha_c) T I}{\Delta T}, \quad (53)$$

where

$$K_s = \frac{K_2 K_1}{K_1 + K_2}. \quad (54)$$

Under open circuit condition, $I_{eq} = 0$, so that, $\Delta V = -\alpha_{eq} \Delta T$. Applying this result, we have for I :

$$I = \frac{1}{R_s + R_c} (\alpha_s - \alpha_c) \Delta T. \quad (55)$$

Using this last result in Eq. (53), we have:

$$K_{eq-PSC} = K_s + K_c + (\alpha_s - \alpha_c)^2 T \frac{1}{R_s + R_c}. \quad (56)$$

Now, we can write the figure of merit for this PSC-CTEG system:

$$Z_{eq-PSC} = \frac{\alpha_{eq-PSC}^2}{R_{eq-PSC} K_{eq-PSC}}. \quad (57)$$

Using the results obtained in Eqs. (48), (51), and (56), we have:

$$Z_{eq-PSC} = \frac{\left(\frac{R_c \alpha_s + R_s \alpha_c}{R_s + R_c}\right)^2}{\left[\frac{R_s R_c}{R_c + R_s}\right] \left[K_s + K_c + (\alpha_s - \alpha_c)^2 T \frac{1}{R_s + R_c}\right]}. \quad (58)$$

6.1.3. Analysis of equivalent figure of merit for composite systems

Equivalent figure of merit (Z_{eq}) is calculated in this section for TES and PSC systems. For performing calculations, the best known thermoelectric materials for commercial applications have been selected: BiTe, PbTe, and SiGe (experimental data taken from Refs. [14–16] have been used as numerical values of thermoelectric parameters). It has also been calculated equivalent maximum efficiency (η_{eq-max}).

It is important to emphasize, that in this study we analyzed also the behavior of Z_{eq} and η_{eq} when ordering of materials in the composite system changes (i.e., change its position).

Table 2 shows, that performance of composite system is affected by the type of thermal and electrical connection, as well as ordering of materials. For example, PSC case reaches the highest value of Z_{eq} and η_{eq} with the ordering $TEG 1 = PbTe$, $TEG 2 = SiGe$, $TEG 3 = BiTe$.

To analyze the performance of the composite system, with each of the different orderings, we have built plots (**Figure 5a, b**), that show variation of equivalent figure of merit with Seebeck coefficients ratio α_j/α_i .

6.2. Maximum efficiency

The figure of merit measures the performance of materials in thermoelectric device, but, if we measure the performance when the TEG is operating under a temperature difference, then the value called thermal efficiency quantifies the ability of TEG to utilize the supplied heat effectively.

TEG 1	TEG 2	TEG 3	Z_{eq-TEs}	Z_{eq-PSC}	η_{eq-TEs}	η_{eq-PSC}
BiTe	PbTe	SiGe	0.000433	0.000463	0.079936	0.084392
PbTe	SiGe	BiTe	0.000508	0.001905	0.091045	0.224724
SiGe	BiTe	PbTe	0.000574	0.000622	0.100217	0.106658

Table 2. Numerical values of Z_{eq} and η_{eq} in each equivalent thermoelectric system for different arrangements of the TE materials.

From thermodynamics, Carnot cycle thermal efficiency is known as:

$$\eta_{Carnot} = \frac{T_{hot} - T_{cold}}{T_{hot}} \quad (59)$$

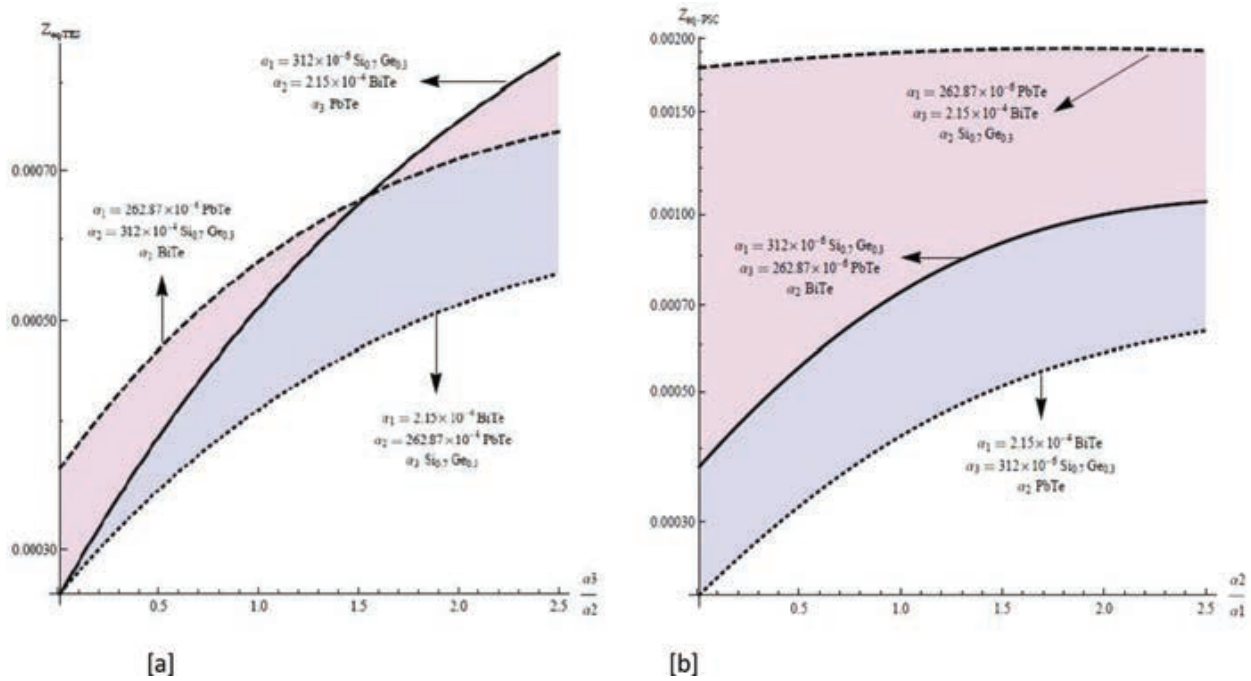


Figure 5. (a) Z_{eq-TES} vs. ratio α_3/α_2 , maintaining α_1 and α_2 constant; (b) Z_{eq-PSC} vs. ratio, α_2/α_1 , maintaining α_1 and α_3 constant.

In terms of η_{Carnot} and Z_{eq} , the maximum efficiency of thermoelectric device is defined by the next equation (with thermoelectric properties (α, R, κ) constant with respect to temperature) [2]:

$$\eta_{max-j} = \frac{\Delta T}{T_{hot}} \cdot \frac{\sqrt{1 + Z_{eq-j} \bar{T}} - 1}{\sqrt{1 + Z_{eq-j} \bar{T}} + \frac{T_{cold}}{T_{hot}}}, \quad (60)$$

where Z_{eq-j} with $j = TES, PSC$ is given by Eqs. (45) and (58), respectively. Thus, we have for the maximum efficiency of TES-CTEG system:

$$\eta_{eq-TES} = \frac{\Delta T}{T_{hot}} \cdot \frac{\sqrt{1 + Z_{eq-TES} \bar{T}} - 1}{\sqrt{1 + Z_{eq-TES} \bar{T}} + \frac{T_{cold}}{T_{hot}}}. \quad (61)$$

For the maximum efficiency of PSC-CTEG system:

$$\eta_{eq-PSC} = \frac{\Delta T}{T_{hot}} \cdot \frac{\sqrt{1 + Z_{eq-PSC} \bar{T}} - 1}{\sqrt{1 + Z_{eq-PSC} \bar{T}} + \frac{T_{cold}}{T_{hot}}}. \quad (62)$$

Our results are shown in **Figure 6**.

Plots in **Figure 6** show typical dependences of CTEGs efficiency on the properties of component materials. The presented results of maximum efficiency reached by the thermoelectric

device approach the limit established by Bergman's theorem for composite materials [17]: the efficiency of composite thermoelectric system cannot be greater than the module's component with highest efficiency.

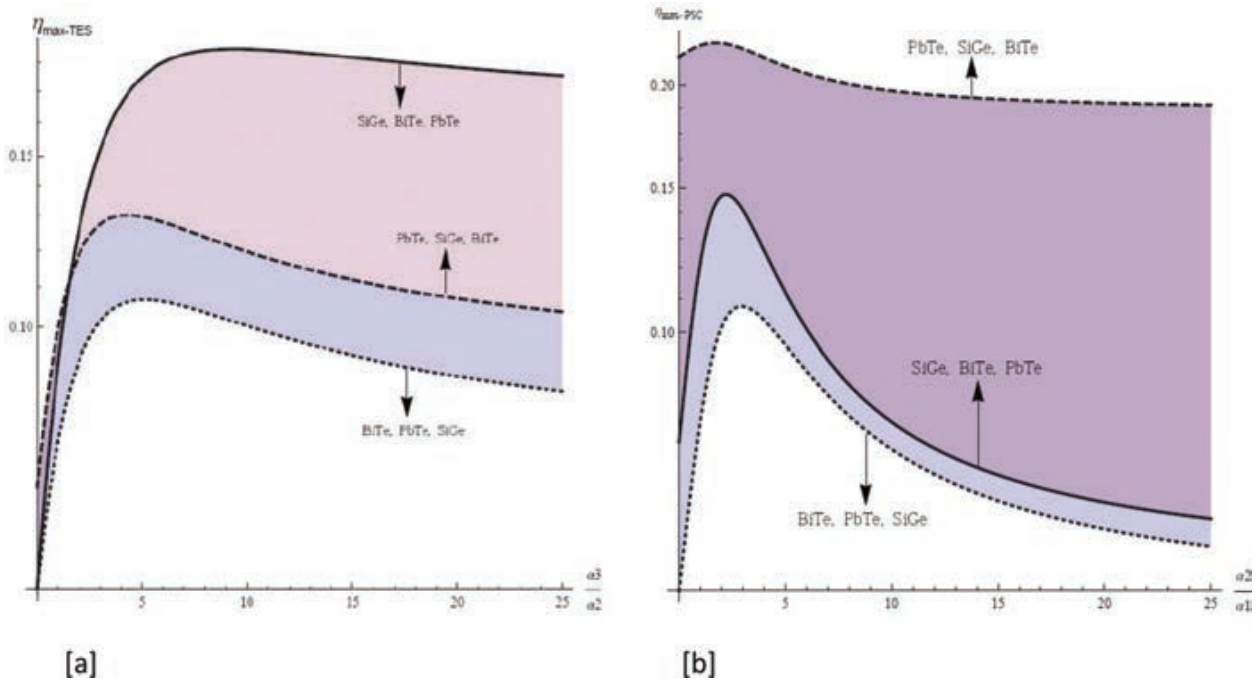


Figure 6. (a) $\eta_{max-TEG}$ vs. ratio α_3/α_2 . (b) $\eta_{max-PSC}$ vs. ratio α_2/α_1 .

The maximum efficiencies achieved by studied CTEGs, see plots in **Figure 6**, are of similar order of magnitude as CTEG systems investigated in some works, e.g. [18], where reported efficiencies from 17 to 20%.

6.3. CTEG: maximum output power

We analyze also the maximum output power of the studied CTEG system, again, assuming configurations and physical conditions shown in Section 6. The obtained results have been compared with some analytical work and numerical simulations.

For the case of thermoelectric generator connected to load resistor R_{load} (**Figure 7**), the power delivered to R_{load} is given by the following equation [19]:

$$P_{out-m} = \frac{[\alpha(T_H - T_C)]^2 m}{(m + 1)^2 R}, \quad (63)$$

The strategy consists of defining the optimal ratio $m = R_{load}/R$ and then by applying the method of maximizing variable to obtain the value of the load resistance, which maximizes power. It yields $R_{load} = R$, and in this case, the maximum output power is:

$$P^{max} = \frac{\alpha^2 (T_H - T_C)^2}{4R}. \quad (64)$$

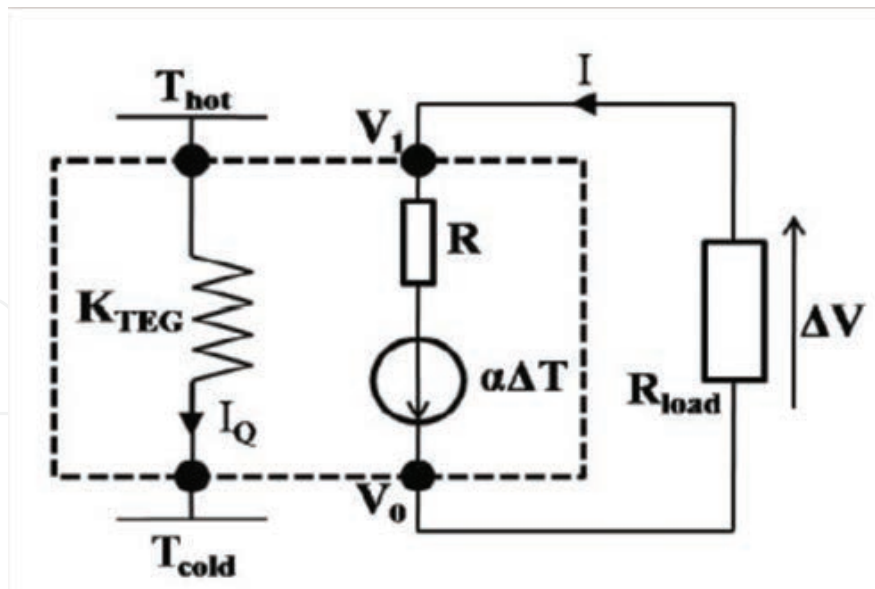


Figure 7. Thermal-electrical circuit for TEG delivering power to the load, where ΔV is the voltage, R_i is the electrical resistance, K_i is the thermal conductance, T_{cold} is the temperature of the cold side, T_{hot} is the temperature of the hot side, ΔT is the temperature difference, α_i is Seebeck coefficient, R_{load} is the load resistance.

6.3.1. Formulation of output power for CTEG

Here, in similar way as in previous sections, formulating of output power will be considered using thermoelectric equivalent quantities, see Sections 6.1.1, 6.1.2 [20]. Thus, using Eqs. (62, 63) in terms of α_{eq} and R_{eq} , we can write:

$$P_{\text{out-}eq\text{-}m} = \frac{[\alpha_{eq}(T_H - T_C)]^2}{R_{eq}} \frac{m}{(m + 1)^2}, \quad (65)$$

$$P_{eq}^{\text{max}} = \frac{\alpha_{eq}^2 (T_H - T_C)^2}{4R_{eq}}. \quad (66)$$

Application of the formalism described above Eqs. (64, 65) give the output power for each configuration as follows.

Two-stage thermoelectric system connected in series:

$$P_{\text{out-}eq\text{-(TES-CTEG)-}m} = \frac{\left(\left[\frac{-(\alpha_2 + \alpha_3)K_1 - \alpha_1 K_2 - \alpha_1 K_3}{K_1 + K_2 + K_3} \right] (T_H - T_C) \right)^2}{\left[R_1 + R_2 + R_3 + \frac{(\alpha_1 - \alpha_2 - \alpha_3)^2 T}{K_1 + K_2 + K_3} \right]} \frac{m}{(m + 1)^2} \quad (67)$$

and the maximum power is given by:

$$P_{eq\text{-(TES-CTEG)}}^{\text{max}} = \frac{\left(\left[\frac{-(\alpha_2 + \alpha_3)K_1 - \alpha_1 K_2 - \alpha_1 K_3}{K_1 + K_2 + K_3} \right] (T_H - T_C) \right)^2}{4 \left[R_1 + R_2 + R_3 + \frac{(\alpha_1 - \alpha_2 - \alpha_3)^2 T}{K_1 + K_2 + K_3} \right]}. \quad (68)$$

Segmented-conventional thermoelectric system in parallel (PSC-CTEG):

$$P_{out-eg-(PSC)-m} = \frac{\left(R_c \left[\frac{K_2 \alpha_1 + K_1 \alpha_2}{K_1 + K_2} \right] + \left[R_1 + R_2 + \left[\frac{(\alpha_1 - \alpha_2)^2 \bar{T}}{K_1 + K_2} \right] \right) \alpha_c \right)^2 (T_H - T_C)^2}{\left[\left[R_1 + R_2 + \frac{(\alpha_1 - \alpha_2)^2 \bar{T}}{K_1 + K_2} \right] R_c (R_s + R_c) \right]} \frac{m}{(m + 1)^2}, \quad (69)$$

and using Eqs. (51, 48) and Eq. (66), the maximum power of this system obtained is:

$$P_{eq-(PSC)}^{max} = \frac{1}{4} \frac{\left(R_c \left[\frac{K_2 \alpha_1 + K_1 \alpha_2}{K_1 + K_2} \right] + \left[R_1 + R_2 + \left[\frac{(\alpha_1 - \alpha_2)^2 \bar{T}}{K_1 + K_2} \right] \right) \alpha_c \right)^2 (T_H - T_C)^2}{\left[\left[R_1 + R_2 + \frac{(\alpha_1 - \alpha_2)^2 \bar{T}}{K_1 + K_2} \right] R_c (R_s + R_c) \right]}. \quad (70)$$

6.3.2. Analysis of output power

We show the behavior of the electrical output power delivered in each CTEG configuration using the data of Section 6.1.3. **Figure 8**, panels (a) and (b), shows the output power as a function of the ratio between the electrical resistance of the load and the electrical resistance of the thermoelectric system $m = \frac{R_{load}}{R}$.

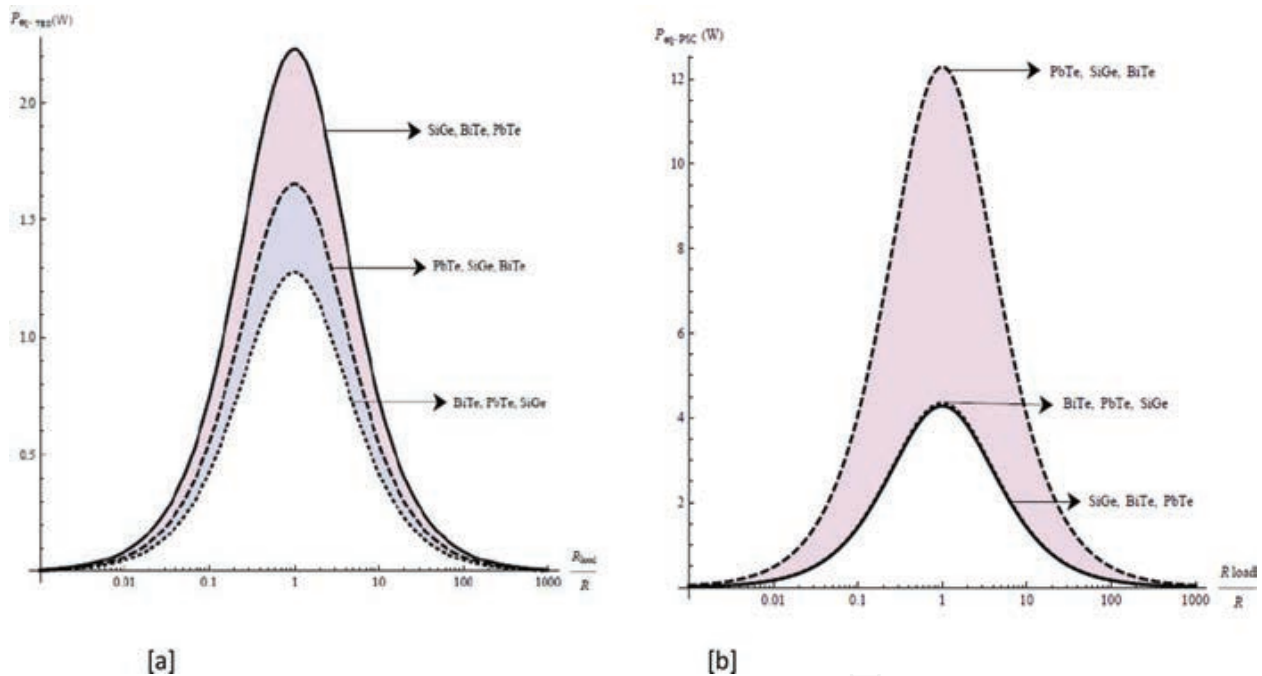


Figure 8. (a) Plot for output power delivered by TES-CTEG system as function of ratio R_{load}/R ; combination, producing the highest output power, is (TEM 1=SiGe, TEM 2=BiTe, TEM 3=PbTe); (b) plot for output power delivered by the PSC-CTEG system as function of ratio R_{load}/R ; combination, producing the highest output power, is (TEM 1=PbTe, TEM 2=SiGe, TEM 3=BiTe).

Plots in **Figure 8** show, that similarly to the equivalent figure of merit and equivalent efficiency (Sections 6.1.3 and 6.2), the output power of a composite system is also influenced by the type of thermal-electrical connection and ordering of materials, and again, PSC-CTEG case shows the highest performance quantified by generated output power. This result is consistent with the results obtained by Vargas-Almeida et al. [20], and the behavior of the output power for

each array of equivalent TES-CTEG is consistent with the results obtained by Apertet et al. [11]. **Table 3** shows the comparison of maximum output power values for different types of connections and possible arrangements.

TEG 1	TEG 2	TEG 3	$P_{max-eq-TEs}$	$P_{max-eq-PSC}$
BiTe	PbTe	SiGe	1.27618	4.34854
PbTe	SiGe	BiTe	1.65563	12.2877
SiGe	BiTe	PbTe	2.22968	4.28067

Table 3. Numerical values of maximum output power, in terms of equivalent amounts of each compound of CTEG, evaluated for each order of building TEGs.

To confirm the validity of our results, we have built plots for CTEG output power using ΔT values of some work: [21] (experimental) and [22, 23] (analytical). Plots in **Figure 9** were produced using the temperature difference of Ref. [21].

The results for comparisons with [22, 23] are shown in [24].

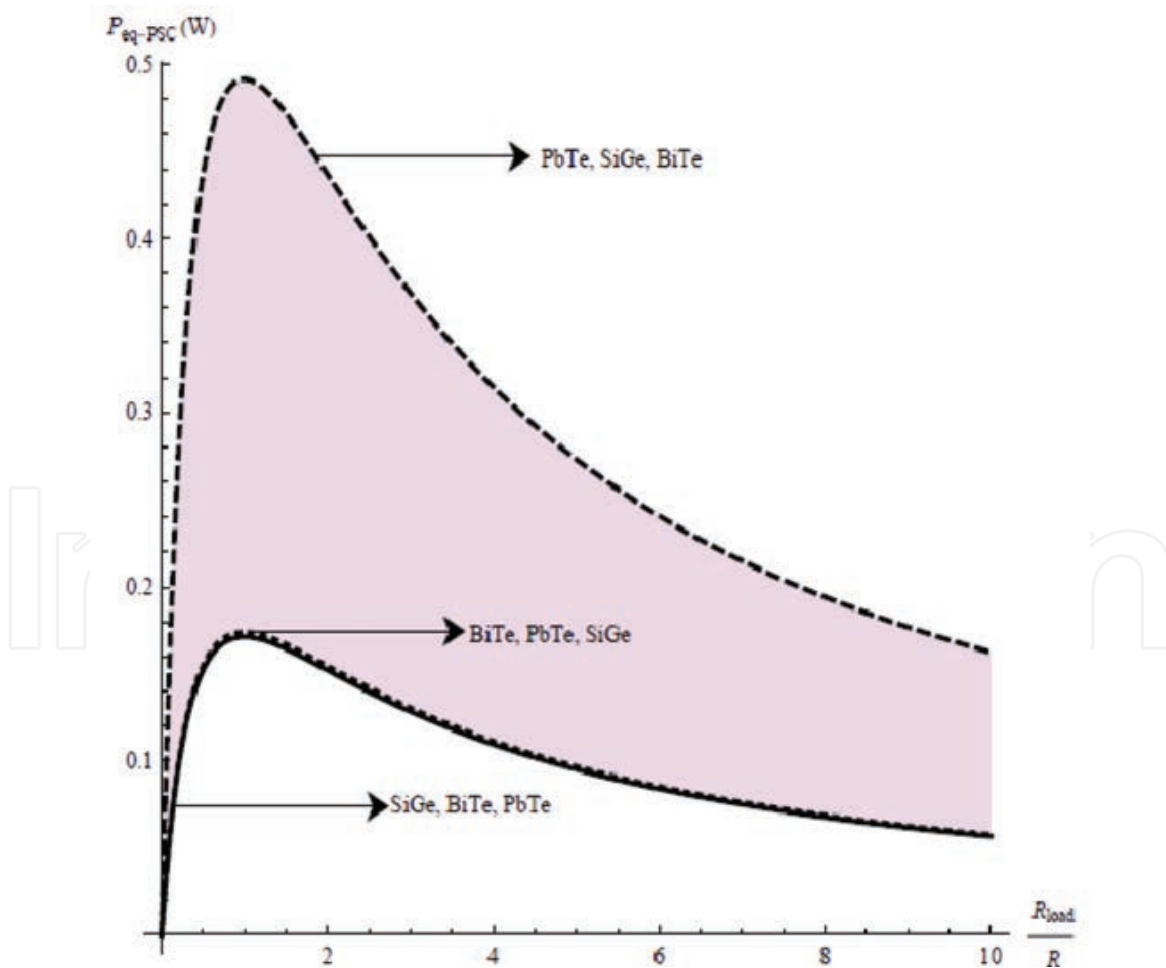


Figure 9. Output power $P_{Out-eq-PSC}$ delivered by composed PSC system vs ratio R_{load}/R . At temperature difference $\Delta T = 20K$, curves behave similarly to the plots shown in Ref. [21]. This figure is consistent with the result obtained by Abdelkefi [21]. Our results have also been compared to other published works [22, 23].

7. Opportunity analysis to improve CTEG design by varying configuration

In this section, we generalize results shown in previous sections by formulating corollary and including some results with realistic approaches, for example, consideration of contact thermal conductance. To achieve this goal, we combine physical conditions imposed in Section 6 with the next options: (1) the whole system is formed of the same thermoelectric material ($\alpha_1, K_1, R_1 = \alpha_2, K_2, R_2 = \alpha_3, K_3, R_3$); (2) the whole system is constituted by only two different thermoelectric materials ($\alpha_i, K_i, R_i = \alpha_j, K_j, R_j \neq \alpha_l, K_l, R_l$), where i, j, l can be 1, 2 or 3, [25].

7.1. Case A: homogeneous thermoelectric properties, configuration effect

We consider configurations of CTEG with the same thermoelectric material, $(\alpha_1, K_1, R_1) = (\alpha_2, K_2, R_2) = (\alpha_3, K_3, R_3)$. In this case, equivalent figure of merit Z_{eq}^h is as follows,

for homogeneous TES-CTEG:

$$Z_{eq-TES}^h = \frac{\left(\frac{-4\alpha_i}{3}\right)^2}{\left(\frac{(-\alpha_i)^2 T}{3K_i} + 3R_i\right)\left(\frac{2K_i}{3}\right)}, \quad (71)$$

for homogeneous PSC-CTEG:

$$Z_{eq-PSC}^h = \frac{(\alpha_i)^2}{\left(\frac{2R_i}{3}\right)\left(\frac{3K_i}{2}\right)}, \quad (72)$$

where $i = (BiTe, PbTe, SiGe)$.

Table 4 shows numerical values of equivalent figure of merit Z_{eq}^h obtained by us for CTEG with considered configurations.

Material	Z_{eq-TES}^h	Z_{eq-PSC}^h
BiTe	0.00212133	0.00305269
PbTe	0.00055109	0.000657238
SiGe	0.000287562	0.00033337

Table 4. Numerical values of Z_{eq}^h for each of three configurations with different materials.

It is important to note, that fulfillment condition $TEG 1 = TEG 2 = TEG 3$ evidences the fact, that although composite system is made of single material, the figure of merit reaches different values depending on type of connection.

7.2. Case B: two different materials in CTEG

CTEG is made of two same materials and the other one different. Thus, two TEGs include same semiconductor material and the other one different semiconductor material. In this case, equivalent figure of merit Z_{eq}^h is as follows, for heterogeneous TES-CTEG:

$$Z_{eq- TES}^{Inh} = \frac{\left(\frac{-(\alpha_j + \alpha_i)K_i - \alpha_i(K_j + K_l)}{K_i + K_j + K_l}\right)^2}{\left(\frac{(\alpha_i - \alpha_j - \alpha_l)^2 T}{K_i + K_j + K_l} + R_i + R_j + R_l\right) \left(\frac{K_i(K_j + K_l)}{K_i + K_j + K_l}\right)}, \quad (73)$$

for heterogeneous PSC-CTEG:

$$Z_{eq-PSC}^{Inh} = \frac{\left(\frac{R_l \left(\frac{K_j \alpha_i + K_i \alpha_j}{K_i + K_j}\right) + \left(R_i + R_j + \frac{(\alpha_i - \alpha_j)^2 T}{K_i + K_j}\right) \alpha_l}{R_i + R_j + R_l + \frac{(\alpha_i - \alpha_j)^2 T}{K_i + K_j}}\right)^2}{\left(\frac{R_l \left(R_i + R_j + \frac{(\alpha_i - \alpha_j)^2 T}{K_i + K_j}\right)}{R_i + R_j + R_l + \frac{(\alpha_i - \alpha_j)^2 T}{K_i + K_j}}\right) \left(\frac{K_j K_i}{K_i + K_j} + K_l + \left(\frac{K_j \alpha_i + K_i \alpha_j}{K_i + K_j} - \alpha_l\right)^2 \frac{T}{R_i + R_j + R_l + \frac{(\alpha_i - \alpha_j)^2 T}{K_i + K_j}}\right)}. \quad (74)$$

Eqs. (72) and (73) are applied with condition $TEG_i = TEG_j$, that is, two TEGs are made of the same thermoelectric material, and third TEG_l is made of different thermoelectric material. Thus, we have three possibilities ($TEG_1 = TEG_2 \neq TEG_3$, $TEG_1 = TEG_3 \neq TEG_2$, $TEG_2 = TEG_3 \neq TEG_1$) for each configuration [25]. Note that, each arrangement has six different combinations, if the cyclical order of the material is taken into account.

The behavior of the equivalent figure of merit as a function of the ratio of the thermal conductivities of the two component materials is shown in **Figure 10**. This step is important, because it shows numerical values, that CTEG maker must meet for both component materials to reach the highest value of Z_{eq} .

Table 5 shows maximum values of equivalent figure of merit of CTEG with material arrangements in every configuration, when $TEG_i = TEG_j \neq TEG_l$.

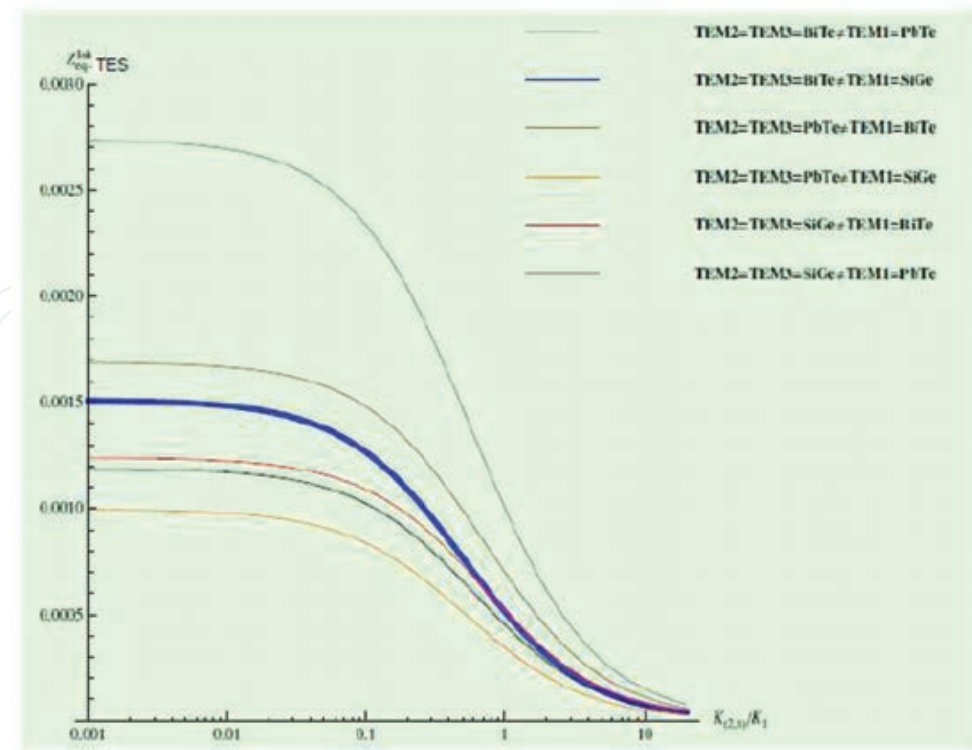
Table 6 shows each configuration with the most efficient material arrangements for every TEG.

Results show again, that the most efficient system of three configurations is PSC with corresponding material arrangement, namely $TEG_1 = TEG_2 = PbTe \neq TEG_3 = BiTe$; see **Figure 11**.

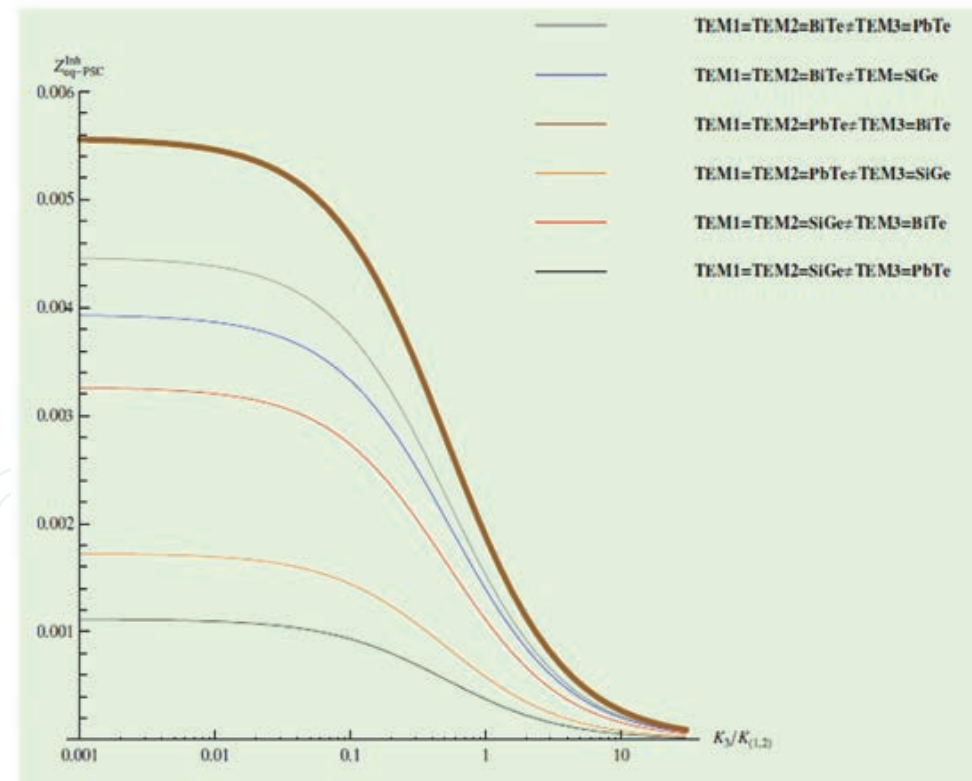
Again, it is important to note, that this result proves, that although the performance of composite systems is affected by combination of different materials, it is affected by the position of such materials in the system structure as well.

7.3. Performance analysis with realistic approximations

The results of the previous sections have argued, that application of output power and efficiency as quantities to measure performance of the system is reasonable; however, in this new section, we extend the analysis of these quantities using realistic considerations. Numerical treatment is performed with Z_{eq-PSC}^{Inh} .



[a]



[b]

Figure 10. (a) Equivalent figure of merit for heterogeneous TES-CTEG, under condition $TEG\ 2=TEG\ 3\neq\ TEG\ 1$, the highest numerical value is corresponding to $TEG\ 2=TEG\ 3=BiTe\neq\ TEG\ 1=PbTe$; (b) Equivalent figure of merit for heterogeneous PSC-CTEG under condition $TEG\ 1=TEG\ 2\neq\ TEG\ 3$, the highest numerical value is corresponding to $TEG\ 1=TEG\ 2=PbTe\neq\ TEG\ 3=BiTe$.

TEG 1	TEG 2=TEG 3	$Z_{eq-TEs-max}^{Inh}$
BiTe	PbTe	0.00168734
BiTe	SiGe	0.0012388
PbTe	BiTe	0.00273649
PbTe	SiGe	0.00118802
SiGe	BiTe	0.00150947
SiGe	PbTe	0.000994534
TEG 3	TEG 1=TEG 2	$Z_{eq-PSC-max}^{Inh}$
BiTe	PbTe	0.0055567
BiTe	SiGe	0.00325841
PbTe	BiTe	0.00445846
PbTe	SiGe	0.0011157
SiGe	BiTe	0.00392902
SiGe	PbTe	0.00172358

Table 5. Maximum values of equivalent figure of merit of CTEG with material arrangements in every configuration, when $TEM_i = TEM_j \neq TEM_l$.

System	Arrangement
TES	TEG 2=TEG 3=BiTe≠TEG 1=PbTe
PSC	TEG 1=TEG 2=PbTe≠TEG 3=BiTe

Table 6. Most efficient material arrangements $TEG_i = TEG_j \neq TEG_l$ for TES and PSC-CTEG systems.

7.3.1. Maximum output power

In the following analysis, we consider thermoelectric modules as isolated units only. Although this is usually considered as an ideal situation, such an approach is useful to study the performance of materials in the composite system. However, for real applications, modules must be coupled to heat exchangers, which produces thermal conductance of contact (K_c) at the coupling points. This affects system performance and reflects in the output power. Here, the maximum output power is calculated using the maximum value of the equivalent figure of merit (Z_{eq-PSC}^{Inh}) [23]:

$$P_{max-PSC} = \frac{(K_c \Delta T)^2}{4(K_{I=0} + K_c) \bar{T}} \frac{Z_{eq-PSC}^{Inh} \bar{T}}{1 + Z_{eq-PSC}^{Inh} \bar{T} + K_c / K_{I=0}} \quad (75)$$

Figure 12a shows maximum output power values for PSC system as function of ratio $K_{I=0}/K_c$, that is, in terms of internal thermal conductance $K_{I=0}$ and contact thermal conductance K_c , under condition $TEG 1=TEG 2 \neq TEG 3$.

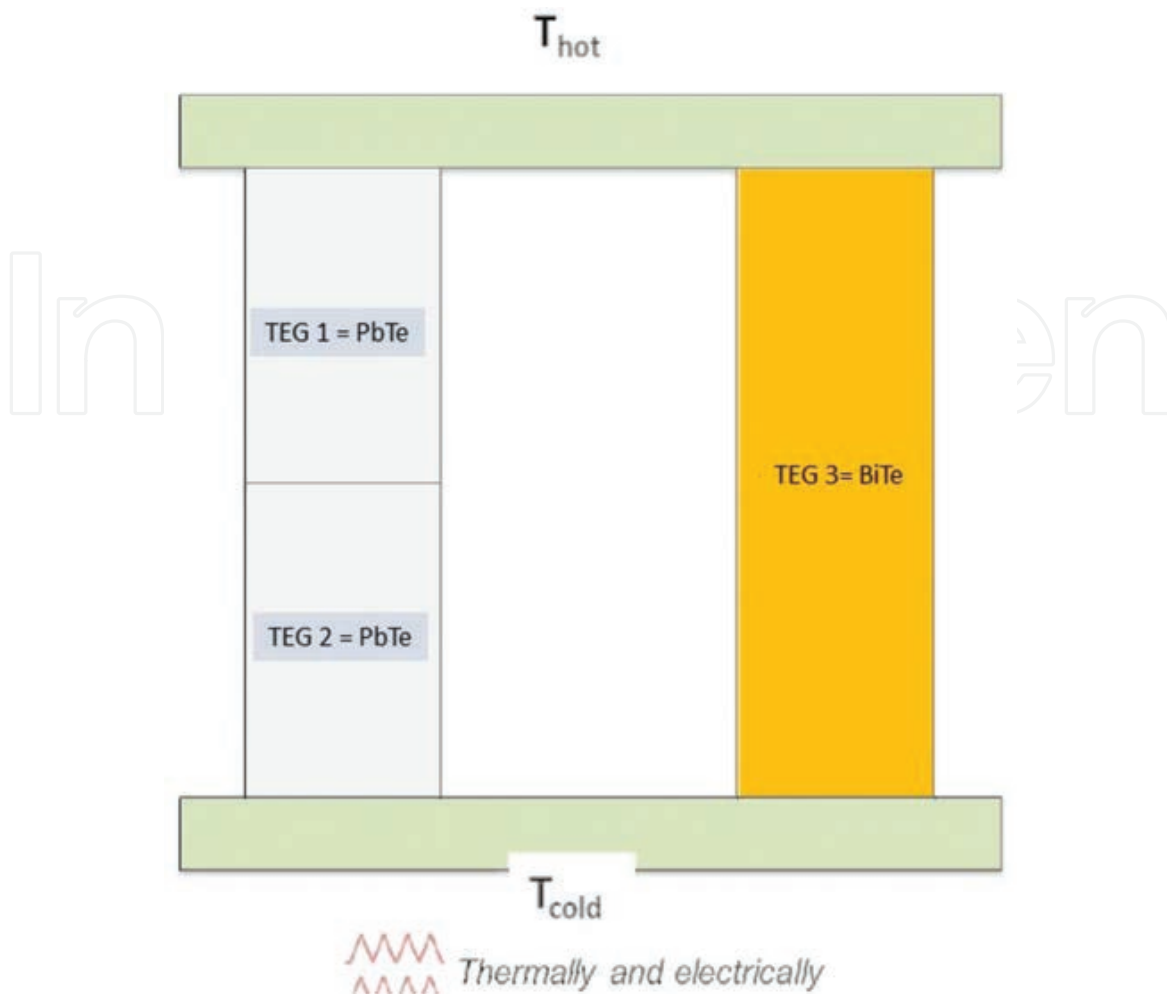


Figure 11. Optimal configuration corresponds to PSC-CTEG with arrangement TEG 1=TEG 2=PbTe≠TEG 3=BiTe.

7.3.2. Efficiency

To calculate the efficiency of PSC systems with TEG 1=TEG 2=PbTe≠TEG 3=BiTe arrangement, we applied the equation:

$$\eta_{eq-PSC}^{Inh} = \frac{\Delta T}{T_H} \frac{\sqrt{1 + Z_{eq-PSC}^{Inh} \bar{T}} - 1}{\sqrt{1 + Z_{eq-PSC}^{Inh} \bar{T} + \frac{T_C}{T_H}}} \quad (76)$$

Finally, for an ideal TEG, that is, without taking into account heat exchangers, we can analyze TEG efficiency considering intrinsic thermal conductances ratio ($K_3/K_{1,2}$) and electrical resistances ratio ($R_3/R_{1,2}$).

Figure 12b shows contour plot for different values of η_{eq-PSC}^{Inh} as function of ratios, $K_3/K_{1,2}$ and $R_3/R_{1,2}$. We can see, that the range of optimal values for the best efficiency of PSC–CTEG lies in intervals 0.1–1.0 and 0.1–0.5 for $K_3/K_{1,2}$ and $R_3/R_{1,2}$, respectively. It is remarkable, that thermal conductances ratio shows a wider range of good values in comparison with electrical resistances ratio, which shows narrower range.

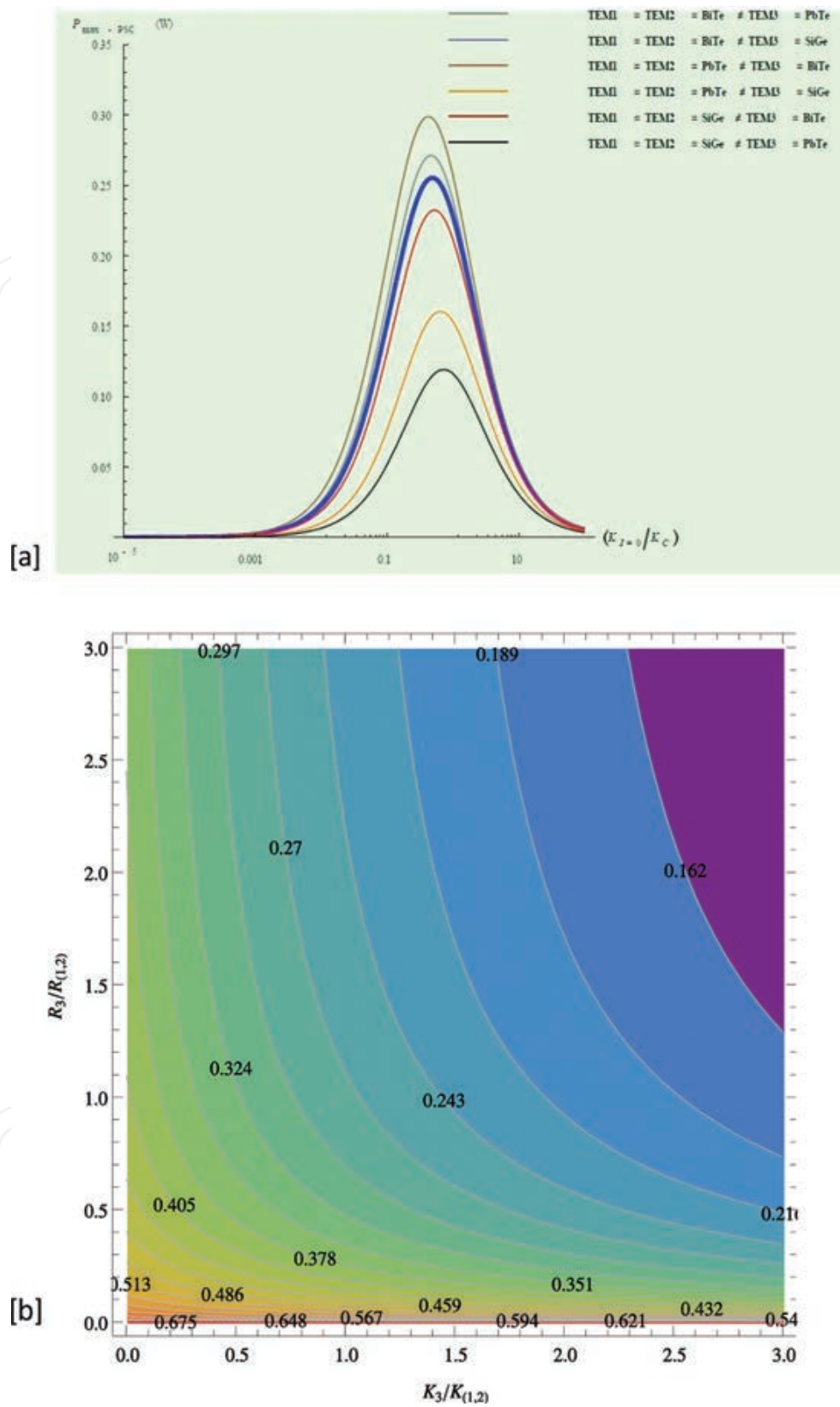


Figure 12. (a) Maximum power of PSC system under condition $TEG\ 1=TEG\ 2\neq TEG\ 3$, the highest numerical value corresponding to arrangement $TEG\ 1=TEG\ 2=PbTe\neq TEG\ 3=BiTe$. (b) Contour plot: efficiency of PSC system under condition $TEG\ 1=TEG\ 2\neq TEG\ 3$, assuming the maximum value of efficiency Z_{eq-PSC}^{Inh} for arrangement $TEG\ 1=TEG\ 2=PbTe\neq TEG\ 3=BiTe$.

7.3.3. Corollary: maximum efficiency Z_{eq} for composite thermoelectric generator

Based on the progress presented in this paper, we have been formulated the following corollary: two features of design must be met to ensure the maximum value of Z_{eq} of CTEG:

- If the material is the same in all components, CTEG reaches the maximum value of Z_{eq} with a specific type of thermal–electrical connection.
- When components of TEGs composing CTEG are made of different materials, $TEG_i \neq TEG_j \neq TEG_l$ where $i; j; l$ can be 1, 2, or 3; then, for a given thermal-electrical connection, there exists an optimal arrangement of thermoelectric materials for which Z_{eq} is maximum.

8. Conclusions

The main objective of this chapter was to present new ideas for designing more complex thermoelectric systems taking into account the effects of electrical and thermal connection, combination of different materials and ordering of materials in CTEG. For this purpose, we considered the framework of linear response theory for nonequilibrium thermodynamic processes, and we used the constant parameter model. Through the definition of equivalent parameters α_{eq} , R_{eq} , and K_{eq} , we have shown the significant impact of these parameters on the system's properties, which characterize the performance of CTEG, namely Z_{eq} , η_{eq} , and P_{eq} . The numerical results show, that the optimal configuration for CTEG considered here is the thermal and electrical connection in parallel with arrangement (*PbTe*, *SiGe* and *BiTe*). For completeness, we have shown the effect of contact thermal conductance on the parameter Z_{eq-PSC}^{Inh} for the most efficient case—*PSC-CTEG* system, in terms of both ratio $K_3/K_{1,2}$ (intrinsic thermal conductances) and $R_3/R_{1,2}$ (intrinsic electrical resistance). Although in this study, the composite system is restricted to only three components, the results can be generalized to systems consisting of N modules, either analytically by extension of the mathematical model or through numerical simulations; guidelines for this purpose are provided by the corollary 7.3.3.

Author details

Alexander Vargas Almeida¹, Miguel Angel Olivares-Robles^{2*} and Henni Ouerdane^{3,4}

*Address all correspondence to: molivares67@gmail.com

1 Departamento de Termofluidos, Facultad de Ingenieria, Universidad Nacional Autonoma de Mexico, Mexico

2 Instituto Politecnico Nacional, SEPI-Esime Culhuacan, Coyoacan, Ciudad de Mexico, Mexico

3 Russian Quantum Center, Skolkovo, Moscow Region, Russian Federation

4 UFR Langues Vivantes Etrangeres, Universite de Caen Normandie, Esplanade de la Paix, Caen, France

References

- [1] Apertet Y, Ouerdane H, Goupil C, Lecoer Ph: A note on the electrochemical nature of thermoelectric power. *EPJ Plus*. 2016;131:76. doi:10.1140/epjp/i2016-16076-8
- [2] Ioffe AF: *Semiconductor Thermoelements and Thermoelectric Cooling*. London: Infosearch; 1957.
- [3] Seebeck TJ: *Treatises Royal Academy of Sciences*, Berlin. 1821:289.
- [4] Peltier JCA: *Annals of Chemical Physics*. 1834;56:371–386.
- [5] Pottier N: *Out-of-equilibrium statistical physics, linear irreversible processes irréversibles linéaires*. Paris: EDP Sciences/CNRS Editions: 2007.
- [6] Callen HB: The application of Onsager's reciprocal relations to thermoelectric, thermomagnetic, and galvanomagnetic effects. *Phys. Rev.* 1948;73:1349–1358. doi:10.1103/PhysRev.73.1349
- [7] Onsager L. Reciprocal relations in irreversible processes. I. *Phys. Rev.* 1931;37:405–426. doi:10.1103/PhysRev.37.405
- [8] Onsager L. Reciprocal relations in irreversible processes. II. *Phys. Rev.* 1931;38:2265–2279. doi:10.1103/PhysRev.38.2265
- [9] Domenicali CA. Irreversible thermodynamics of thermoelectricity. *Rev. Mod. Phys.* 1954;26:237–275. doi:10.1103/RevModPhys.26.237
- [10] Callen HB. *Thermodynamics and an introduction to thermostatistics*, 2nd revised ed. New York: John Wiley & Sons; 1985.
- [11] Apertet Y, Ouerdane H, Goupil C, Lecoer Ph. Internal convection in thermoelectric generator models. *J. Phys. Conf. Series*. 2012;395:012103. doi:10.1088/1742-6596/395/1/012103
- [12] Apertet Y, Ouerdane H, Goupil C, Lecoer Ph. Equivalent parameters for series thermoelectrics. *Energy Convers. Manag.* 2015;93:160–165. doi:10.1016/j.enconman.2014.12.07
- [13] Apertet Y, Ouerdane H, Goupil C, Lecoer PH. Thermoelectric internal current loops inside inhomogeneous systems. *Phys. Rev. B*. 2012;85:033201. doi:10.1103/PhysRevB.85.033201
- [14] Hsu CT, Huang GY, Chu HS, Yu B, Yao DJ. An effective Seebeck coefficient obtained by experimental results of a thermoelectric generator module. *Appl. Energy*. 2011;88:5173–5179. doi:10.1016/j.apenergy.2011.07.33
- [15] Barron KC. *Experimental studies of the thermoelectric properties of microstructured and nanostructured lead salts*. [Bachelor's thesis]. Cambridge: Massachusetts Institute of Technology; 2005, p. 28.
- [16] Hurwitz EN, Asghar M, Melton A, Kucukgok B, Su L, Oroc M, Jamil M, Lu N, Ferguson IT. Thermopower study of GaN-based materials for next-generation thermoelectric devices and applications. *J. Electron. Mater.* 2011;40:513–517. doi:10.1007/s11664-010-1416-9

- [17] Shakouri A. Recent developments in semiconductor thermoelectric physics and materials. *Annu. Rev. Mater. Res.*. 2011;41:399–431. doi:10.1146/annurev-matsci-062910-100445
- [18] Ouyang Z, Li D. Modelling of segmented high-performance thermoelectric generators with effects of thermal radiation, electrical and thermal contact resistances. *Sci. Rep.* 2016;6:24123. doi:10.1038/srep24123. .
- [19] Goupil C, Seifert W, Zabrocki K, Muller E, Snyder GJ. Thermodynamics of thermoelectric phenomena and applications. *Entropy*. 2011;3:1481–1517. doi:10.3390/e13081481
- [20] Vargas A, Olivares MA, Camacho P. Thermoelectric system in different thermal and electrical configurations: its impact on the figure of merit. *Entropy*. 2013;15:2162–2180. doi:10.3390/e15062162
- [21] Abdelkefi A, Alothman A, Hajj MR. Performance analysis and validation of thermoelectric energy harvesters. *Smart Mater. Struct.* 2013;22:095014. doi:10.1088/0964-1726/22/9/095014
- [22] Nemir D, Beck J. On the significance of the thermoelectric figure of merit *Z*. *J. Electron. Mater.* 2010;39:1897–1901. doi:10.1007/s11664-009-1060-4
- [23] Apertet Y, Ouerdane H, Glavatskaya O, Goupil C, Lecoœur P. Optimal working conditions for thermoelectric generators with realistic thermal coupling. *EPL*. 2012;97:28001. doi:10.1209/0295-5075/97/28001
- [24] Vargas A, Olivares MA, Camacho P. Maximum power of thermally and electrically coupled thermoelectric generators. *Entropy*. 2014;16:2890–2903. doi:10.3390/e16052890
- [25] Vargas A, Olivares MA, Mendez Lavielle F. Performance of composite thermoelectric generator with different arrangements of SiGe, BiTe and PbTe under different configurations. *Entropy*. 2014;16:2890. doi:10.3390/e17117387

IntechOpen